



Short communication

Excellent dispersion and electrocatalytic properties of Pt nanoparticles supported on novel porous anatase TiO₂ nanorods

Xun Guo^a, Dao-Jun Guo^{a,b}, Xin-Ping Qiu^{a,*}, Li-Quan Chen^a, Wen-Tao Zhu^a^a Key Laboratory of Organic Optoelectronics and Molecular Engineering, Department of Chemistry, Tsinghua University, Beijing 100084, PR China^b School of Chemistry and Chemical Engineering, Qufu Normal University, Qufu, Shandong 273165, PR China

ARTICLE INFO

Article history:

Received 19 May 2009

Accepted 20 May 2009

Available online 27 May 2009

Keywords:

Methanol electro-oxidation

Carbon monoxide tolerance

Porous nanorods

Titanium dioxide

Pt nanoparticles

Direct methanol fuel cells

ABSTRACT

We synthesize, for the first time, a new Pt based catalyst for direct methanol fuel cells using home-made novel porous anatase TiO₂ nanorods as a new catalyst support. Pt nanoparticles are prepared by an improved ethylene glycol reduction method and supported on the surface of TiO₂ with excellent dispersion and without any aggregates. The structure and elemental composition of the TiO₂ and Pt/TiO₂ catalyst are characterized by transmission electron microscopy (TEM), nitrogen sorption, energy-dispersive X-ray spectroscopy (EDS) and X-ray diffraction (XRD). The electrocatalytic properties of the Pt/TiO₂ catalyst for methanol and carbon monoxide electro-oxidation reactions are investigated by cyclic voltammetry (CV) in an acidic medium. Apparent electrocatalytic activity for methanol electro-oxidation reaction, high carbon monoxide tolerance and good stability are all observed for the Pt/TiO₂ catalyst. These may be attributed to the excellent dispersion of the Pt nanoparticles and the special properties of the TiO₂ support. These results imply that this Pt/TiO₂ catalyst has promising potential applications in direct methanol fuel cells.

© 2009 Published by Elsevier B.V.

1. Introduction

Direct methanol fuel cells (DMFCs) have been considered the ideal clean and mobile fuel cell system for portable electronic devices and transportation applications, because they are superior to other kinds of fuel cells in terms of weight–volume energy densities, working conditions and so on [1,2]. In an acidic medium, the most efficient catalyst for DMFC is a platinum (Pt) based catalyst. The electrocatalytic activity of catalysts for methanol electro-oxidation is dependent on many factors [3,4]. Of these, the catalyst support and its surface condition are essential for the catalyst to increase its electrocatalytic activity [5,6]. In previous studies, a variety of carbon supports have been investigated based on their high chemical stability and good electron conductivity and so on [7–10]. However, because of their hydrophobicity, it is difficult to disperse Pt nanoparticles on them. Some papers have reported using oxidizing acid or surfactant in a pretreatment step to improve their surface condition. However, this procedure is complicated and it is still difficult to get good dispersion of the Pt nanoparticles.

Novel porous anatase TiO₂ nanorods were recently reported by Bao et al. [11]. The results of SEM and TEM analysis indicated that the TiO₂ nanorods have a large specific surface area and a porous

structure, both of which are important in the field of electrocatalytic applications [12,13] because of advantages in terms of mass transport and co-catalytic effects. Hence, in this work and for the first time, we report on a new Pt based catalyst using novel porous anatase TiO₂ nanorods as catalyst support. We have tested its electrocatalytic properties and stability as a promising potential anodic electrocatalyst for DMFCs.

2. Experimental

2.1. Preparation of Pt/TiO₂ catalyst

The porous anatase TiO₂ nanorods support material was prepared by a simple approach, followed by sintering at 500 °C, which is described in detail elsewhere [11]. Pt nanoparticles were supported on porous TiO₂ nanorods by an improved simple one-step EG method. The results of our experiments have shown that porous anatase TiO₂ nanorods which were sintered at 300 °C will decompose in the EG reduction step. This is presumed to be caused by the lower sintering temperature. In a typical process, the appropriate quantity of H₂PtCl₆·6H₂O in ethylene glycol solution (0.02 M) was mixed with NaOH in ethylene glycol solution (0.1 M). The ethylene glycol serves as a stabilizer and reducing agent. Porous TiO₂ nanorods were then added to the mixed solution and sonicated for 15 min and the solution stirred at 130–140 °C for 4 h. The reaction mixture was cooled to room temperature and dripped with

* Corresponding author. Tel.: +86 10 62794234; fax: +86 10 62794234.

E-mail address: qiuXP@mails.tsinghua.edu.cn (X.-P. Qiu).

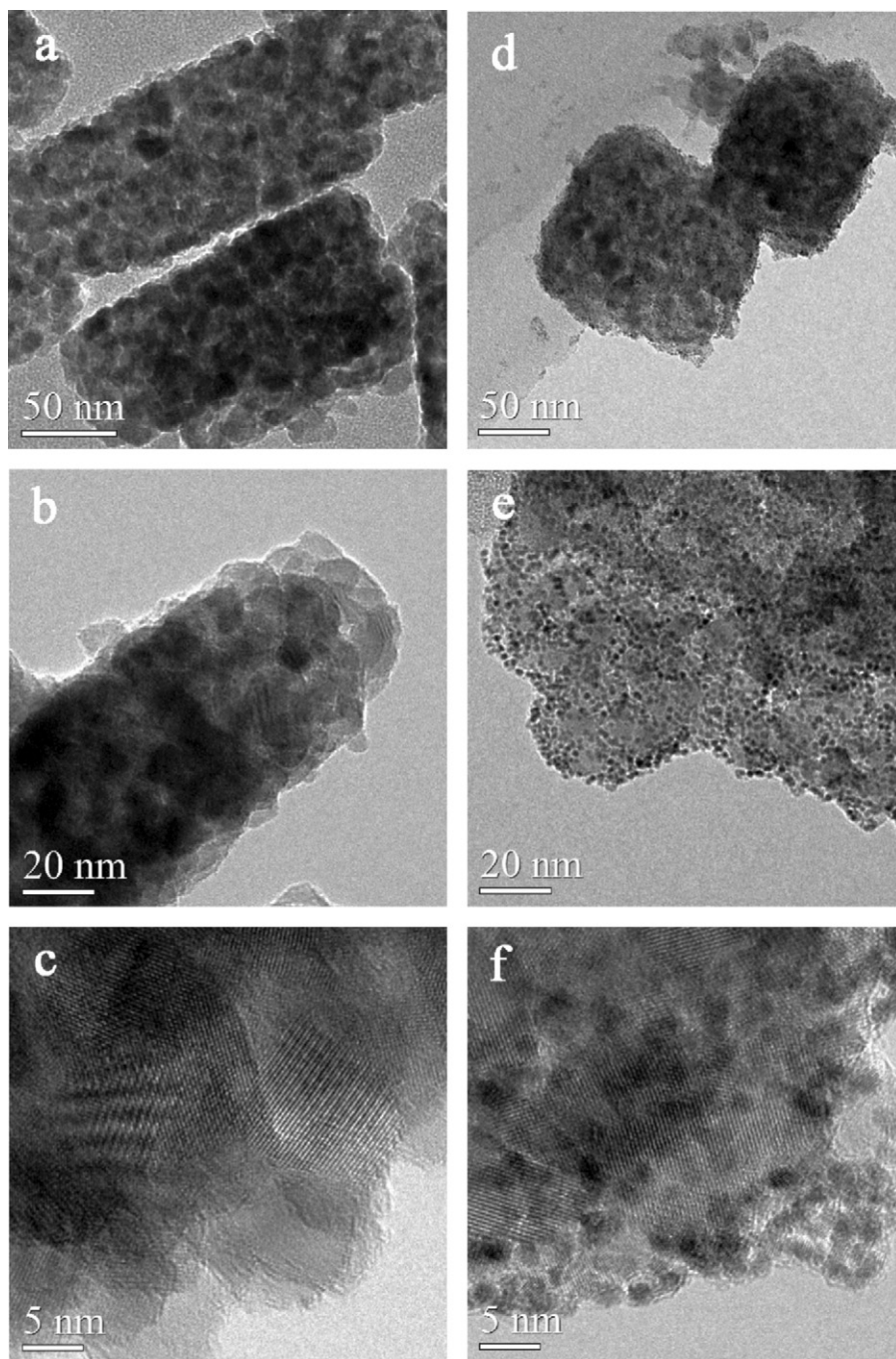


Fig. 1. TEM images of TiO_2 and the Pt/ TiO_2 catalyst: (a, b, and c) TiO_2 ; (d, e, and f) Pt/ TiO_2 .

KNO_3 (0.1 M) and HCl (0.5 M) successively for 4 h. After stirring overnight, the product was collected by centrifugation, washed several times with H_2O and ethanol, and dried in a vacuum oven at 70°C overnight. From this the Pt/ TiO_2 catalyst was obtained. The Pt was controlled to be 20 wt% in the Pt/ TiO_2 catalyst. Commercial anatase TiO_2 nanoparticles were used in the preparation of porous TiO_2 nanorods without further treatment. A commercial Pt/C catalyst (Pt wt% = 60%, Johnson Matthey) was used in the CO stripping measurement, without further treatment.

2.2. Measurement

The electrochemical activity of the catalysts was measured by cyclic voltammetry (CV) using a three-electrode cell in a PARSTAT

2273 potentiostat controlled by PowerSuite[®] software (Princeton Applied Research). The working electrode was gold plating coated with a thin layer of Nafion-impregnated catalyst. As a typical process, the catalyst ink was prepared by ultrasonic dispersion of about 0.5 mg catalyst in a 15 μL mixture of Nafion solution (20% Nafion and 80% ethylene glycol) and 65 μL DI water for 15 min. After coating the catalyst ink on to a polished planar gold patch (1.0 cm \times 1.0 cm), the electrodes were air-dried at 80°C for 2 h. Pt gauze and a saturated mercurous sulfate electrode ($\text{Hg}/\text{Hg}_2\text{SO}_4$) were used as the counter electrode and reference electrode, respectively. All potentials in this report are quoted vs. $\text{Hg}/\text{Hg}_2\text{SO}_4$. The CV test was conducted at 50 mV s^{-1} in a nitrogen saturated solution of 0.5 M H_2SO_4 with 1 M CH_3OH , with the potential ranging from -0.63 to 0.55 V . The CO stripping test was conducted at 20 mV s^{-1} in a nitrogen saturated

solution of 0.5 M H_2SO_4 , with the potential ranging from -0.63 to 0.55 V. All the electrochemical measurements were conducted at 25°C .

The morphology of the Pt/TiO₂ catalyst was investigated using transmission electron microscopy (TEM, JEOL model JEM-2011) operating at 200 keV. The elemental composition of the Pt/TiO₂ catalyst was investigated using scanning electron microscopy (SEM, JEOL model JEM-6301F) operating at 15 keV and equipped with an energy-dispersive spectrometer (EDS). The X-ray diffraction (XRD) analysis was performed using a Rigaku X-ray diffractometer with a Cu K α radiation source. Values of 2θ between 10° and 90° were scanned at a rate of 8°min^{-1} with a step of 0.02° . The N_2 sorption measurement was performed using Quantachrome QuadraSorb SI at 77.3 K and the specific surface area and pore size distribution were calculated using the Brunauer–Emmett–Teller (BET) and Barrett–Joyner–Halenda (BJH) methods, respectively.

3. Results and discussion

3.1. TEM analysis and elemental composition of Pt/TiO₂ catalyst

TEM images of TiO₂ and the Pt/TiO₂ catalyst are shown in Fig. 1. Fig. 1a and b shows that porous TiO₂ nanorods had been prepared. Fig. 1d and e shows that uniform Pt nanoparticles were deposited on to the surface of the porous TiO₂ nanorods with excellent dispersion and without any aggregation, giving an efficient utilization of Pt. From Fig. 1c and d, the average particle sizes of TiO₂ and Pt nanoparticles were determined to be about 12.2 nm and 2.0 nm, respectively. EDS data confirms the correct stoichiometry of the TiO₂ and Pt/TiO₂ catalyst.

3.2. N_2 sorption and XRD analysis of the Pt/TiO₂ catalyst

The N_2 sorption isotherms of samples were recorded and results are shown in Fig. 2a. Both the TiO₂ and Pt/TiO₂ catalyst show similar isotherm curves with a weak jump at $P/P_0 = 0.3$ – 0.5 and another jump at $P/P_0 = 0.8$ – 0.9 . These jumps are characteristic of porous solids. The data showing specific surface area and corresponding pore sizes and pore volumes are summarized in Table 1. The values of BET specific surface area, pore size and pore volume of the Pt/TiO₂ catalyst are all lower than those of TiO₂. This is due to the fact that the Pt nanoparticles were dispersed within the pores of the porous TiO₂ support, leading to blocking of the pore channels and a consequent decrease of the measured surface area, pore size and pore volume [14].

The XRD patterns of the TiO₂ and Pt/TiO₂ catalyst are shown in Fig. 2c. From the XRD pattern of TiO₂, it can be seen that all of the diffraction peaks correspond to the pure TiO₂ phase, with no impurity peaks, and is in good agreement with the standard spectrum (JCPDS, card no: 21-1272) [7]. From the XRD pattern of the Pt/TiO₂ catalyst, it can be seen that four new diffraction peaks appear, which are in good agreement with the peaks of pure Pt nanoparticles and correspond to the face-centered cubic (fcc) crystal structure [15–17].

3.3. Electrocatalytic properties of the Pt/TiO₂ catalyst

The electrochemical measurements were carried out in a N_2 saturated 0.5 M H_2SO_4 aqueous solution in the absence and presence of 1.0 M methanol, as shown in Fig. 3a and b. Fig. 3a shows the typical cyclic voltammograms (CVs) of TiO₂ and Pt/TiO₂ catalyst in 0.5 M N_2 saturated H_2SO_4 aqueous solutions. From curve 2 in Fig. 3a, the normal hydrogen absorption and desorption peaks can be observed, which is a result of the Pt nanoparticles dispersed on the surface of the TiO₂ support. Fig. 3b shows typical CVs of TiO₂ and the Pt/TiO₂ catalyst in N_2 saturated 0.5 M H_2SO_4 + 1 M CH_3OH aqueous

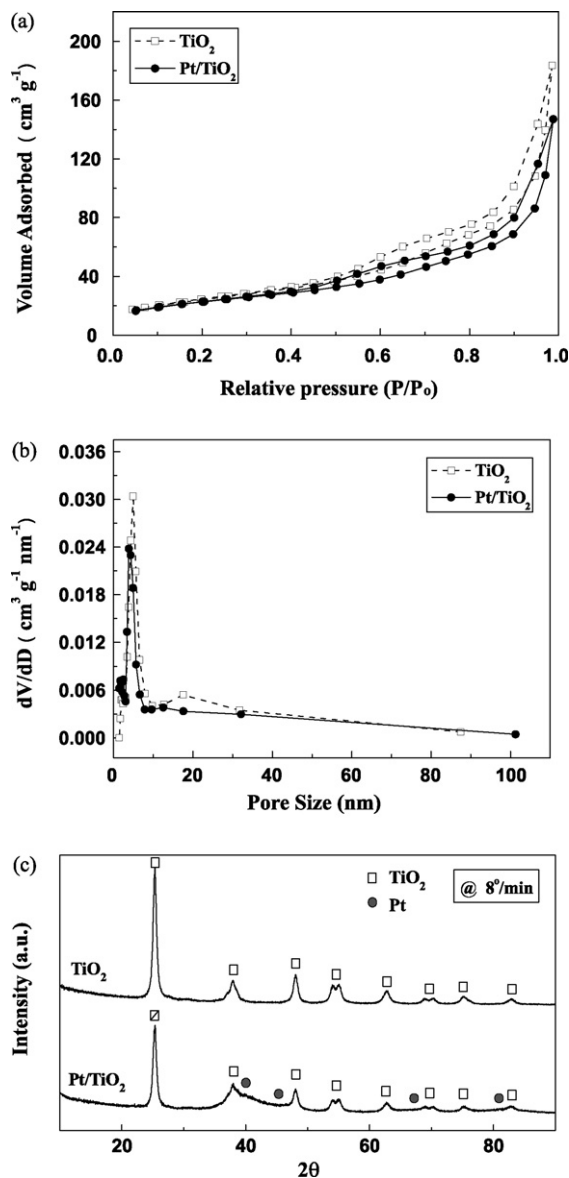


Fig. 2. (a) Nitrogen sorption isotherms, (b) the corresponding pore size distributions and (c) XRD patterns for TiO₂ and the Pt/TiO₂ catalyst.

ous solution. For the TiO₂ electrode, the background current (curve 1), which is capacitive in nature due to the double layer capacitance, is much larger, due to the high surface area of the porous TiO₂ electrode. However, no current peaks of methanol electro-oxidation are observed, which indicates that the TiO₂ has no electrocatalytic activity for the methanol electro-oxidation reaction. From curve 2 in Fig. 3b, two peaks corresponding to methanol electro-oxidation are observed. These two peaks and their onset potentials are at 0.19 V, 0.00 V and -0.32 V, respectively, values which are more negative than those of the other catalysts [18]. This may be attributed to the particular surface properties of the TiO₂ support. We believe that TiO₂ may promote the activity of Pt nanoparticles by accelerating the CO_{ads} electro-oxidation on the surface of Pt according to a bifunctional mechanism, a mechanism which is supported by the CO stripping results.

The CO stripping measurement data of Pt/TiO₂ and Pt/C catalysts was obtained from Fig. 3c and d and are shown in Table 1. From Table 1, a comparison of the CO electro-oxidation curves for both catalysts reveals that the onset and peak potentials of the Pt/TiO₂ catalyst are lower than those of the Pt/C catalyst, which illustrates

Table 1
Pore structure parameters of TiO₂ and Pt/TiO₂ catalyst and CO stripping data of Pt/TiO₂ and Pt/C catalysts.

Sample	BET surface area (m ² g ⁻¹)	BJH pore size (nm)	Pore volume (cm ³ g ⁻¹)	CO stripping ^a	
				Peak potential (V vs. Hg/Hg ₂ SO ₄)	Onset potential (V vs. Hg/Hg ₂ SO ₄)
TiO ₂	88	4.9	0.29		
Pt/TiO ₂	80	3.8	0.23	0.21	0.08
Pt/C				0.36	0.16

^a Obtained from Fig. 3c and d.

the beneficial role of the TiO₂ support for CO electro-oxidation. According to the bifunctional mechanism, TiO₂ can accelerate the CO_{ads} electro-oxidation on Pt, releasing the active sites of Pt for further electrochemical reaction, and hence, the activity of Pt towards methanol electro-oxidation is enhanced [19]. The CO stripping results imply that there may be abundant active hydroxyl groups on the surface of the TiO₂ support, which not only increases the CO tolerance of the Pt/TiO₂ catalyst, but is also because the Pt nanoparticles are supported on the surface of the TiO₂ with excellent dispersion and without any pretreatment.

The long-term stability of the Pt/TiO₂ catalyst was also investigated in N₂ saturated 0.5 M H₂SO₄ + 1 M CH₃OH aqueous solution with the result shown in Fig. 3e. It can be seen that the peak current density decreases gradually with successive scans. The loss of electrocatalytic activity may result from the consumption of methanol during the CV scans. It may also be due to a poisoning effect and the structure change of the Pt nanoparticles as a result of the perturbation of the potentials during the scanning in aqueous

solutions, especially in the presence of organic compounds [20]. After long-term CV experiments, the catalyst layer was not removed from the surface of the gold plate and the integrity of the working electrode was maintained. The Pt/TiO₂ working electrode was stored in distilled water for a week, then methanol electro-oxidation was carried out again by CV; good electrocatalytic activity towards methanol electro-oxidation was still observed. This indicates that the Pt/TiO₂ catalyst prepared in our experiment has good long-term stability and storage properties.

All the results demonstrate the promising potential application of porous TiO₂ nanorods as a new catalyst support, without any pretreatment. It increases the electrocatalytic activity and CO tolerance of the Pt based catalyst and supports more Pt nanoparticles on its surface, with excellent dispersion, according to the bifunctional mechanism [13]. Because TiO₂ is a semiconductor, its electronic conductivity is lower than that of carbon black or carbon nanotubes. Therefore, further research to increase the electron and proton conductivities of Pt/TiO₂ catalyst is currently in progress.

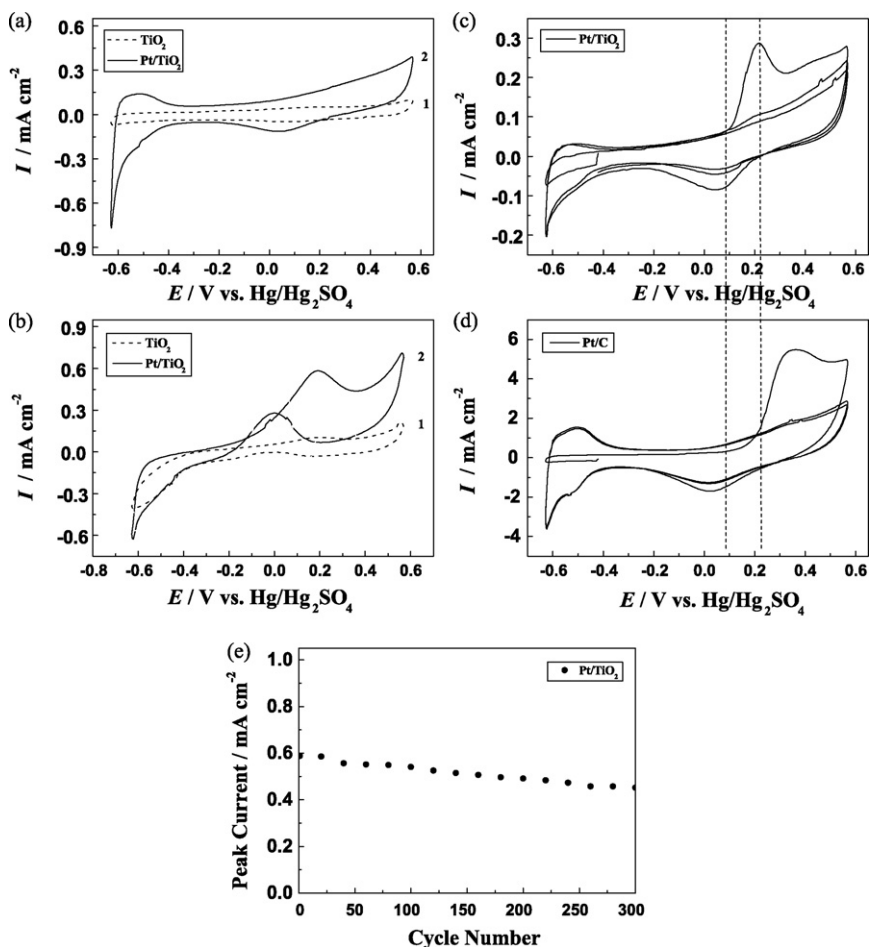


Fig. 3. Electrochemical characterization of TiO₂ and Pt/TiO₂ catalyst: (a) cyclic voltammograms (CVs) of 0.5 M H₂SO₄, scan rate: 50 mV s⁻¹; (b) CVs of 1 M CH₃OH in 0.5 M H₂SO₄, scan rate: 50 mV s⁻¹. CO stripping curves recorded in 0.5 M H₂SO₄ with a scan rate of 20 mV s⁻¹: (c) Pt/TiO₂ catalyst; (d) Pt/C catalyst. (e) Stability of the Pt/TiO₂ catalyst over 300 cycles of methanol electro-oxidation in 0.5 M H₂SO₄ + 1 M CH₃OH. Scan rate: 50 mV s⁻¹.

4. Conclusion

We have synthesized, for the first time, a new Pt based catalyst for DMFCs using homemade novel porous anatase TiO₂ nanorods as the catalyst support. The results of N₂ sorption measurement and TEM analysis have indicated that the TiO₂ support has a large specific surface area and porous structure. The results of CVs show that the Pt/TiO₂ catalyst has apparent electrocatalytic activity for the methanol electro-oxidation reaction. The results of CO stripping measurements indicate that the TiO₂ support can increase the CO tolerance of the Pt based catalyst and support Pt nanoparticles with excellent dispersion, according to the bifunctional mechanism. All the measurements described in the present paper confirm the promising potential applications, in DMFCs, of this new Pt based catalyst with novel porous anatase TiO₂ nanorods as the catalyst support.

Acknowledgements

The authors appreciate the financial support of the State Key Basic Research Program of PRC (2009CB220105) and National Natural Science Foundation of China (90410002).

References

- [1] A. Hamnett, *Catal. Today* 38 (1997) 445.
- [2] B.D. McNicol, D.A.J. Rand, K.R. Williams, *J. Power Sources* 83 (1999) 15.
- [3] A. Kabbabi, F. Gloaguen, F. Andolfatto, R. Durand, *J. Electroanal. Chem.* 373 (1994) 251.
- [4] A. Gamez, D. Richard, P. Gallezot, F. Gloaguen, R. Faure, R. Durand, *Electrochim. Acta* 41 (1996) 307.
- [5] J.S. Yu, S. Kang, S.B. Yoon, G. Chai, *J. Am. Chem. Soc.* 124 (2002) 9382.
- [6] S.J. Dong, Q.H. Qiu, *J. Electroanal. Chem.* 314 (1991) 223.
- [7] R.M. Baum, *Chem. Eng. News* 75 (1997) 39.
- [8] C. Bernard, J.M. Planeix, B. Valerie, *Appl. Catal. A* 173 (1998) 175.
- [9] E. Antolini, *Appl. Catal. B* 88 (2009) 1.
- [10] Y.Y. Shao, J. Liu, Y. Wang, Y.H. Lin, *J. Mater. Chem.* 19 (2009) 46.
- [11] S.J. Bao, Q.L. Bao, C.M. Li, Z.L. Dong, *Electrochem. Commun.* 9 (2007) 1233.
- [12] Y.S. Tao, H. Kanoh, L. Abrams, K. Kaneke, *Chem. Rev.* 106 (2006) 896.
- [13] B. Lee, D. Lu, J.N. Kondo, K. Domen, *J. Am. Chem. Soc.* 124 (2002) 11256.
- [14] X.Z. Cui, J.L. Shi, H.R. Chen, L.X. Zhang, L.M. Guo, J.H. Gao, J.B. Li, *J. Phys. Chem. B* 112 (2008) 12024.
- [15] J. Luo, M.M. Maye, V. Petkov, N.N. Kariuki, L. Wang, P. Njoki, D. Mott, Y. Lin, C.J. Zhong, *Chem. Mater.* 17 (2005) 3086.
- [16] M.L. Wu, D.H. Chen, T.C. Huang, *Chem. Mater.* 13 (2001) 599.
- [17] Z.L. Liu, L.M. Gan, L. Hong, W.X. Chen, J.Y. Lee, *J. Power Sources* 139 (2005) 73.
- [18] J.Y. Xi, J.S. Wang, L.H. Yu, X.P. Qiu, L.Q. Chen, *Chem. Commun.* (2007) 1656.
- [19] C. Roth, N. Benker, Th. Buhrmester, M. Mazurek, M. Loster, H. Fuess, D.C. Koningsberger, D.E. Ramaker, *J. Am. Chem. Soc.* 127 (2005) 14607.
- [20] R. Parsons, T. VanderNoot, *J. Electroanal. Chem.* 257 (1988) 9.